Cell PRESS
Chemistry & Biology
Article

Collapsing the Proton Motive Force to Identify Synergistic Combinations against *Staphylococcus aureus*

Maya A. Farha,[1,2] Chris P. Verschoor,[3] Dawn Bowdish,[3] and Eric D. Brown[1,2,*]
[1]Department of Biochemistry and Biomedical Sciences
[2]Michael G. DeGroote Institute of Infectious Disease Research
[3]McMaster Immunology Research Centre, Department of Pathology and Molecular Medicine
McMaster University, Hamilton, ON L8N 3Z5, Canada
*Correspondence: ebrown@mcmaster.ca
http://dx.doi.org/10.1016/j.chembiol.2013.07.006

SUMMARY

Pathways of bacterial energy metabolism, such as the proton motive force (PMF), have largely remained unexplored as drug targets, owing to toxicity concerns. Here, we elaborate on a methodical and systematic approach for targeting the PMF using chemical combinations. We began with a high-throughput screen to identify molecules that selectively dissipate either component of the PMF, $\Delta\Psi$ or ΔpH, in *Staphylococcus aureus*. We uncovered six perturbants of PMF, three that countered $\Delta\Psi$ and three that selectively dissipated ΔpH. Combinations of dissipators of $\Delta\Psi$ with dissipators of ΔpH were highly synergistic against methicillin-resistant *S. aureus*. Cytotoxicity analyses on mammalian cells revealed that the dose-sparing effect of the observed synergies could significantly reduce toxicity. The discovery and combination of modulators of $\Delta\Psi$ and ΔpH may represent a promising strategy for combating microbial pathogens.

INTRODUCTION

Emergence and spread of multidrug-resistant bacteria represents an increasingly serious problem and an unmet medical need due to the lack of therapeutic options. The situation is especially dire for *Staphylococcus aureus* for which methicillin-resistant *S. aureus* (MRSA) and vancomycin intermediate-resistant *S. aureus* (VISA) strains have emerged (Chopra, 2003). The escalating concern of antibiotic resistance coupled with the dwindling antibiotic pipeline has prompted drug developers to turn to unconventional strategies for the discovery of novel drugs to combat bacterial infections, both in exploring novel compound classes and validating new target pathways.

The cell membrane of *S. aureus*, in particular, is a relatively unexplored target for the development of novel antimicrobials. This essential macromolecular structure plays a critical role in cellular activities such as active transport of substances into the cell, cellular respiration, the establishment of the proton motive force, and cell-cell communication (Hurdle et al., 2011). Yet, over the years, discovery efforts have steered clear of membrane-active agents that either disrupt the membrane's physical integrity or target its energetics, mostly given their propensity to cause toxicity in mammals. In fact, a consensus has emerged in the field that active compounds discovered in whole cells screens that act primarily on the cell membrane should be excluded from further study (O'Neill and Chopra, 2004; Silver, 2011). Indeed, a number of assays have been explored to detect these undesirable compounds early enough to evade follow-up studies (Gentry et al., 2010; Prakash Singh, 2006).

Paradoxically, this unconventional antibacterial target has gained attention, in part because of studies showing its importance in nongrowing bacteria (Coates and Hu, 2008; Hu et al., 2010; Hurdle et al., 2011) and out of recognition of the recent success of the antibiotic medicines daptomycin (Hawkey, 2008), telavancin (Zhanel et al., 2010), and HT61 (Hu et al., 2010), all of which work by permeablizing and depolarizing the cytoplasmic membrane of *S. aureus*. Also noteworthy is the compound TMC107, which disrupts membrane energetics by targeting the ATP synthase and is currently in phase IIb trials for the treatment of drug-resistant *Mycobacterium tuberculosis* (Balemans et al., 2012). Nevertheless, the energetic pathways of the bacterial membrane remain largely unexplored and relatively unpopular drug targets.

In bacteria, the extrusion of protons by the electron transport chain results in an electrochemical gradient of protons, known as the proton motive force (PMF), generated across the cell membrane. The PMF is subsequently necessary for ATP synthesis by the F_1F_0-ATPase and for transport of various solutes (Mitchell, 1966). The PMF is made up of the sum of two parameters: the electric potential ($\Delta\Psi$) and the transmembrane proton gradient (ΔpH). Critical to bacterial survival, the PMF has nevertheless been largely disregarded as a target for antimicrobials, owing to toxicity concerns. Still, ionophores such as the natural product monensin, that dissipate the PMF by disrupting the flow of ions across the membrane, have found extensive use as antibacterial agents in the cattle and poultry industries (Russell and Houlihan, 2003). Interestingly, bacteria exercise exquisite control over $\Delta\Psi$ and ΔpH in order to maintain a constant value of PMF. Dissipation in either component is compensated for by a counteracting increase in the other (Bakker and Mangerich, 1981). In this work, we sought to exploit this compensation mechanism as an Achilles heel in bacteria that would be exquisitely susceptible to a combination of perturbants, one that specifically

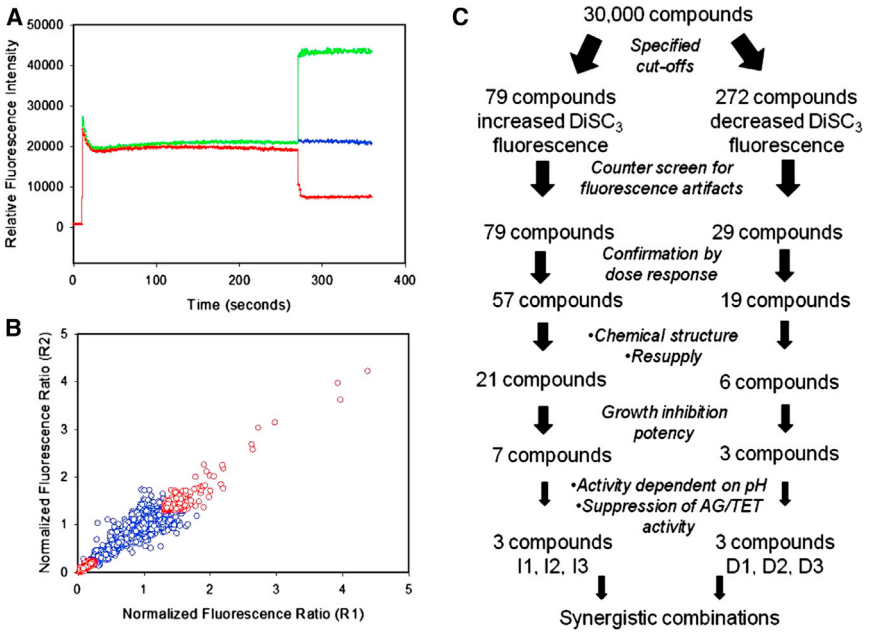

Figure 1. A High-Throughput Screen to Identify Dissipaters of ΔΨ and ΔpH

(A) Fluorescence of $DiSC_3(5)$ over time following addition of DMSO (blue), valinomycin (5 μM), which disrupts ΔΨ (green), and nigericin (5 μM), which disrupts ΔpH (red). $DiSC_3(5)$ dye was first added at 10 s followed by self-quenching and stabilization. Solvent or compounds were added at 270 s.

(B) Replicate plot of the $DiSC_3(5)$ primary screen. *S. aureus* was grown and loaded with $DiSC_3(5)$. Cells were added to one of each of the 30,000 compounds at 10 μM. Shown are the normalized ratios of fluorescence values of two replicate samples. The cutoff score for molecules that increased $DiSC_3(5)$ fluorescence was chosen as $\geq$1.4 and for molecules that decreased fluorescence $\leq$0.25. Active compounds are shown in red.

(C) Schematic diagram of the work flow from the high-throughput screen of 30,000 compounds to yield the active compounds that increased fluorescence, I1, I2, and I3 as well as those that decreased fluorescence, D1, D2, and D3. Compounds were eliminated at each stage according to the criteria indicated. Specifically, after confirming a dose-dependent fluorescence response, the various compounds were tested for the effect of pH on their activity and their ability to suppress the activity of the aminoglycoside (AG), kanamycin, and tetracycline (TET). In aggregate, six compounds were confirmed as modulators of components of PMF. These were investigated for synergistic activity against MRSA.

See also Figures S1–S3.

disrupted the electric potential (ΔΨ) and another, the transmembrane proton gradient (ΔpH).

We set out to identify specific disrupters of the electrical and chemical components of PMF through a fluorescence-based high-throughput screen. In particular, the screen identified three compounds that specifically dissipated ΔΨ and three that selectively disrupted ΔpH. We demonstrated profound synergy between these two classes of compounds when used in combination against MRSA. Thus, the concerted dissipation of ΔΨ and ΔpH had a synergistic effect in collapsing the PMF and, importantly, this synergy spares the doses that are necessary for each of the individual agents. We show that this dose-sparing phenomenon likewise reduces the toxicity of the respective agents. Indeed, drug combination therapy is gaining favor (Keith et al., 2005) because of increased efficacy, lower toxicity, and reduced propensity for resistance (Cottarel and Wierzbowski, 2007). Here, we report on a systematic effort in discovering synergistic antibacterial chemical combinations that exploits the interdependence of the electric potential and chemical gradient of the membrane in maintaining the proton motive force. These findings suggest new opportunities to target energetic systems within bacterial pathogens as a means to develop novel therapeutic strategies.

RESULTS

Development of a High-Throughput Screen for Alterations in PMF

A widely used probe to study the effect of small molecules on membrane potential is the cationic, membrane potential-sensitive dye, 3,3′-dipropylthiacarbocyanine iodide [$DiSC_3(5)$] (Wu et al., 1999). In this fluorescence-based assay, bacteria are grown and loaded with dye, which accumulates in the cytoplasmic membrane in response to ΔΨ and self-quenches its own fluorescence. When ΔΨ is disrupted or the membrane permeabilized upon treatment with a small molecule, the dye is released into the medium resulting in an increase in fluorescence. Interestingly, this dye can also inform on dissipation in the other component of PMF, the transmembrane ΔpH, through observed decreases in fluorescence. Upon dissipation of their pH gradient, bacterial cells will compensate by increasing ΔΨ to maintain a constant PMF. As such, this increased membrane potential further concentrates $DiSC_3(5)$ dye in the membrane, such that high local concentrations lead to decreased fluorescence intensity due to further quenching. As validation for the assay, we measured the effect of valinomycin (in the presence of K^+) and nigericin. Valinomcyin, a K^+ ionophore which specifically dissipates the ΔΨ component of the PMF, led to a significant increase in fluorescence (Figure 1A), whereas nigericin, an electroneutral antiporter for H^+ and K^+, caused a decrease in fluorescence as it selectively dissipates ΔpH (Figure 1A). Solvent (DMSO)-treated $DiSC_3(5)$-loaded cells did not lead to changes in fluorescence consistent with an intact membrane potential (Figure 1A). Having established $DiSC_3(5)$ as a suitable tool to identify molecules that selectively dissipate both components of the PMF, we adapted the methodology to a microwell plate format to allow screening of large numbers of compounds. In this assay, after loading *S. aureus* cells with $DiSC_3(5)$ and treating with compound, dissipation of either ΔΨ or ΔpH was immediate, but stable for at least 30 min, which allowed a sufficient window of time for recording fluorescence intensity. Overall, the optimized $DiSC_3(5)$ microwell assay had robust signal and noise

characteristics, with average Z′ values (Zhang et al., 1999) of 0.88 and 0.80, using known probes valinomycin and nigericin for increases and decreases in fluorescence intensity, respectively.

We carried out a high-throughput screen (HTS) for $DiSC_3(5)$ fluorescence using a diverse collection of synthetic chemicals and known bioactive compounds (30,000 compounds) assayed at 10 μM against *S. aureus* (strain Newman). Results of the screen are shown in Figure 1B, plotted as a normalized fluorescence ratio (see Experimental Procedures) such that a ratio of 1.0 represents no change in fluorescence. We set stringent, arbitrary cutoffs for both increases and decreases in fluorescence as ratios of 1.4 and 0.25, respectively. This translated to 79 compounds that increased fluorescence and 272 compounds that decreased fluorescence (Figure 1C). A counterscreen of the active compounds was conducted to account for fluorescence artifacts, which could arise from intrinsically fluorescent compounds or compounds that quench $DiSC_3(5)$ fluorescence, independent of the proton motive force (Figure S1 available online). The latter effect, assessed by reading the fluorescence intensity in the absence of cells but in the presence of dye, was a very important counterscreen and reduced the number of active compounds that decreased fluorescence to 29. The 79 active compounds that increased $DiSC_3(5)$ fluorescence displayed no fluorescence artifacts (Figure 1C).

Follow-Up to the HTS

In order to confirm active molecules from the HTS, we generated dose response analyses using a range of compound concentrations to assess the dose dependence of the fluorescence readout. Of the 79 compounds that increased fluorescence in the primary screen, 57 dissipated the membrane potential in a concentration-dependent manner (Figure 1C). We eliminated 22 compounds whose effects on $DiSC_3(5)$ fluorescence did not occur in a clear dose-dependent fashion or showed high variability in fluorescence readings among three replicates (examples in Figure S2A). Among the 29 compounds that decreased fluorescence, 19 compounds confirmed as causing a dose-dependent reduction in the pH gradient. Similarly, here, we eliminated ten compounds that did not display clear dose-dependence or exhibited high variability among the three replicates (examples in Figure S2B). Subsequently, we narrowed our list of molecules based on conventional filters, such as visual inspection of chemical structures, ability to resupply, and growth inhibitory potency (detailed process in Figure S3) against *S. aureus*. Although not all dissipaters of components of the PMF have antibacterial activity, we focused on molecules that were inhibitory against *S. aureus*. Importantly, we also observed that antibacterial activity of the molecules against *S. aureus* correlated well with their ability to dissipate either $\Delta\Psi$ or ΔpH. Overall, we narrowed our working set of molecules to ten compounds, seven of which caused an increase in fluorescence ("I" molecules) and potential dissipaters of $\Delta\Psi$ and three causing a decrease in dye fluorescence ("D" molecules), potentially dissipating ΔpH (Figure 1C).

Uncovering Agents that Selectively Dissipate Components of PMF

The nature of the screen not only allows for the discovery of molecules that selectively dissipate components of the PMF, but also agents that permeabilize the membrane allowing $DiSC_3(5)$ dye to be released. Further, because PMF is generated by the electron transport chain, inhibitors of this respiration process may also be uncovered in the screen. It was therefore important to further investigate the mode of action of the active compounds to ensure selective disruption of components of the PMF. To this end, we first assessed the impact of pH on the activity of these compounds. Because the two components of the PMF, the membrane potential and the transmembrane pH gradient (the difference between the intracellular and extracellular pH) are interdependent, a shift in the extracellular pH to alkaline values leads to a decrease in the pH gradient across the membrane, such that the compensatory component, $\Delta\Psi$, accounts for a greater share of the PMF (Booth, 1985). In contrast, a shift to acidic values leads to an increase in ΔpH across the membrane resulting in a compensatory fall in $\Delta\Psi$, such that ΔpH becomes the dominant component (Booth, 1985). A shift in pH to alkaline values led to potentiation of the antibacterial activity of I1, I2, and I3 but did not enhance the activity of the four remaining I molecules, suggesting the former molecules selectively modulate $\Delta\Psi$. The chemical structures of I1, I2, and I3 are shown in Figure 2A along with their $DiSC_3(5)$ dose-response curves in Figure 2B. Specifically, a range of pH 5.5 to pH 9.5 led to a 32-fold change in the minimum inhibitory concentration (MIC) of molecule I1 (Figure 2Ci), a 64-fold shift for I2 (Figure 2Cii), and a 16-fold change for I3 (Figure 2Ciii). Conversely, the antibacterial activity of D1, D2, and D3, for which chemical structures and dose-response curves are shown in Figure 3, increased as pH values became more acidic, consistent with selective disruption of ΔpH. D1 exhibited a 16-fold change in MIC (Figure 3Ci), whereas D2 and D3 showed a 32-fold (Figure 3Cii) and an 8-fold change in MIC (Figure 3Ciii) from a pH range of 9.5 to 5.5, respectively. To further corroborate that the effects of I1-I3 and D1–D3 are specific to components of PMF, we tested their interactions with the aminoglycoside antibiotic kanamycin, whose uptake is driven by $\Delta\Psi$ (Taber et al., 1987), and with tetracycline, whose uptake is specifically driven by ΔpH (Yamaguchi et al., 1991). Indeed, molecules I1–I3 antagonized the activity of kanamycin consistent with the hypothesis that these compounds perturb $\Delta\Psi$. Further, D1–D3 suppressed the activity of tetracycline against *S. aureus* supporting the conclusion that these molecules act on ΔpH (Table S1). As confirmation for the interplay between $\Delta\Psi$ and ΔpH, those molecules that potentiated aminoglycoside activity clearly also suppressed tetracycline action and vice-versa (Table S2).

Thus molecules I1–I3 and D1–D3 represented strong candidate perturbants of $\Delta\Psi$ and ΔpH, where the ultimate goal was testing their efficacy in combination against *S. aureus*. Regarding the remaining molecules, I4–I7, that showed no pH dependency and did not show signature antagonism with kanamycin, we posited that these likely disrupted membrane structure or inhibited other aspects of bacterial respiration. Indeed, we tested these hypotheses as described below.

Characterizing I1, I2, and I3, Potential Dissipaters of $\Delta\Psi$

To further characterize the action of I1, I2, and I3, the potential modulators of $\Delta\Psi$, we first assessed their impact on the energetic condition of *S. aureus* cells by measuring their effect on the reduction of iodonitrotetrazolium chloride (INT). INT, a

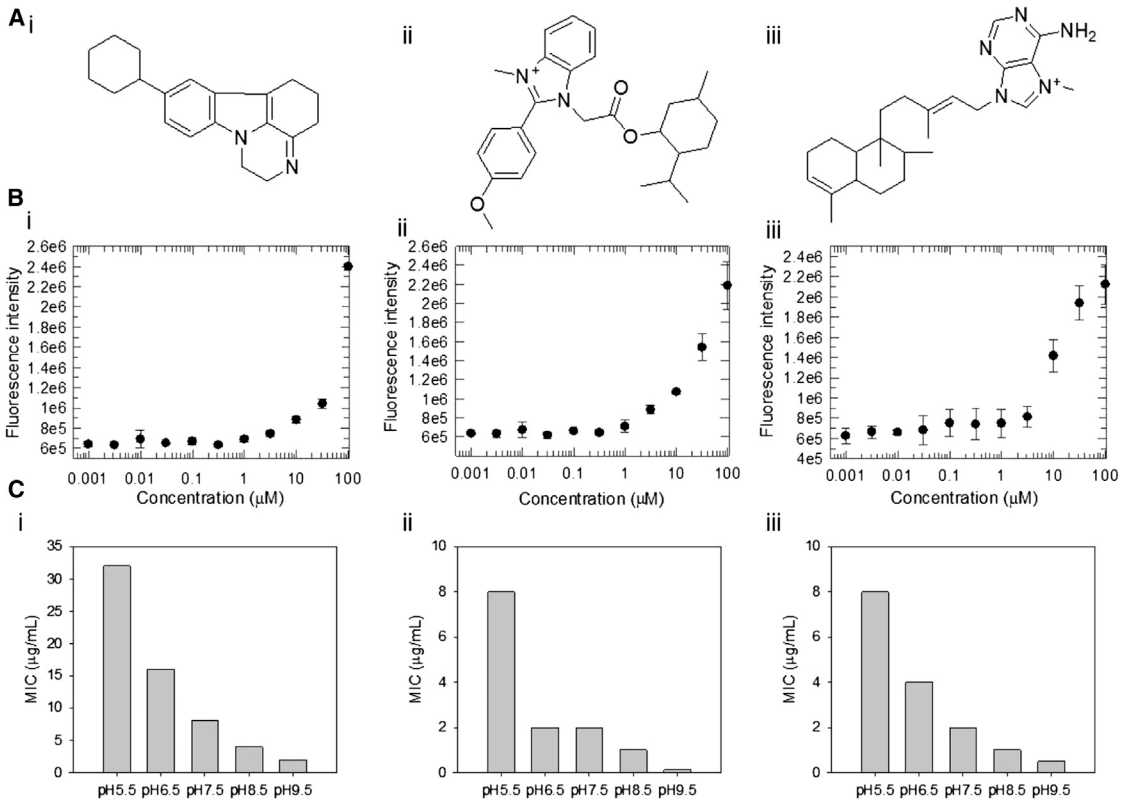

Figure 2. Hit Compounds I1, I2, and I3 Dissipate ΔΨ of *S. aureus*

(A) Chemical structures of (i) I1 (logP = 4.02), (ii) I2 (logP = 2.65), and (iii) I3 (logP = 1.56).

(B) Concentration-dependent effect of (i) I1, (ii) I2, and (iii) I3 on $DiSC_3(5)$ fluorescence. All three compounds caused a dose-dependent increase in fluorescence, indicative of dissipation of ΔΨ. Error bars represent the SEM of three replicates.

(C) The effect of altering the external pH on the minimum inhibitory concentration of (i) I1, (ii) I2, and (iii) I3 is shown. The growth inhibitory activity of all three compounds is enhanced in when the external pH is shifted to an alkaline environment, where ΔΨ becomes the main component of PMF.

See also Tables S1 and S2.

tetrazolium salt, can be reduced to a red insoluble formazan (INF) by components of the prokaryotic respiratory chain (Altman, 1976). Because PMF and the ETC are closely interlinked, whereby generation of an electrochemical proton gradient occurs as a result of the extrusion of protons by the electron transport chain, we reasoned that dissipation of this gradient across the cytoplasmic membrane should ultimately affect electron transport across the respiratory chain. Overall, when tested at concentrations equivalent to their MICs, all three molecules led to significant decreases in the reduction of INT to its formazan product as compared to the untreated control, suggesting that the electron transport across the cytoplasmic membrane was impaired (Figure 4A).

We next investigated the extent to which I1, I2, and I3, by dissipating the membrane potential, interfere with respiratory ATP production. The proton motive force is essential for the production of ATP via the F_0F_1-ATPase, such that dissipation of this electrochemical gradient should halt ATP production. Intracellular ATP levels were measured by a luciferin-luciferase bioluminescence assay at the MIC values of the various compounds. As depicted in Figure 4B, upon addition of I1, intracellular ATP levels drastically decreased by ~84% compared to DMSO-treated control. Similarly, I2 decreased ATP levels by ~41%, whereas I3 decreased ATP levels by 81% compared to the control. This is consistent with a mode of action of dissipating ΔΨ; upon treatment with the various molecules, the intracellular ATP pool is depleted in an attempt to maintain the PMF. These results also suggest that interference with ATP synthesis or depletion of the cellular ATP pool may be the cause of bacterial killing of these molecules as single agents.

We further assessed whether treatment with I1, I2, and I3 results in the efflux of cell constituents by measuring for any loss of materials absorbing at 260 nm. Leakage of cellular constituents, such as potassium ions, amino acids, and ATP, is a common mechanism shared by many small molecules that dissipate PMF. Although some cause pores (Garcerá et al., 1993; McAuliffe et al., 1998), others integrate in the membrane (Silverman et al., 2003; Ultee et al., 1999), similar to an ionophore-like inhibitor and cause dissipation of the ion gradients. In this assay, molecules I2 and I3 did not cause a leak of cellular constituents, as compared to the DMSO control (Figure 4C). Nisin, a pore-forming lantibiotic (Garcerá et al., 1993), served as a positive control and led to a significant increase in absorbance, consistent with its mode of action. I1 caused an intermediate absorbance at a concentration equivalent to its MIC (Figure 4C). This increased absorbance is likely attributable to I1's high

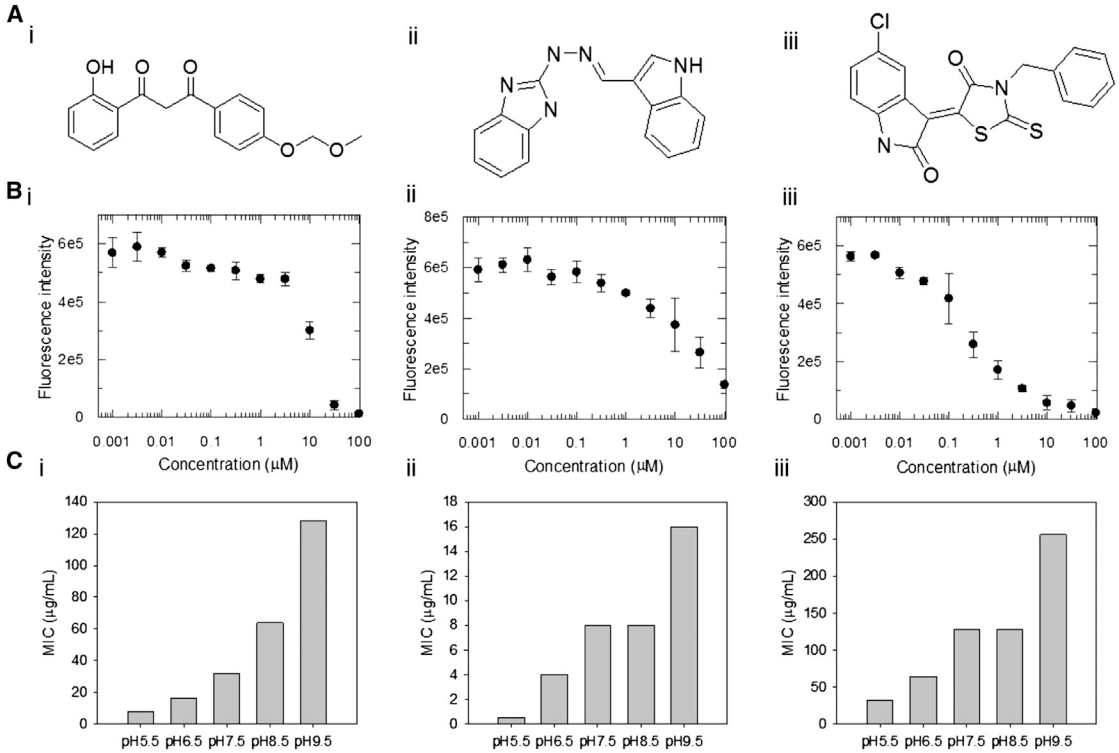

Figure 3. Hit Molecules D1, D2, and D3 Dissipate ΔpH of *S. aureus*

(A) Chemical structures of (i) D1 (logP = 2.33), (ii) D2 (logP = 2.72), and (iii) D3 (logP = 3.02).

(B) Concentration-dependent effect of (i) D1, (ii) D2, and (iii) D3 on $DiSC_3(5)$ fluorescence. All three compounds caused a dose-dependent decrease in fluorescence, indicative of dissipation of ΔpH. Error bars represent the SEM of three replicates.

(C) The effect of altering the external pH on the minimum inhibitory concentration of (i) D1, (ii) D2, and (iii) D3 is shown. The growth inhibitory activity of all three compounds is enhanced in when the external pH is shifted to an acidic environment, where ΔpH becomes the main component of PMF.

See also Tables S1 and S2.

hydrophobicity, which may favor its partitioning into the cytoplasmic membrane, consequently dissipating the transmembrane ion gradient. Nucleic acids, which were leaked through a damaged cytoplasmic membrane, were more abundant with increased concentrations of I1 (data not shown), presumably as more I1 dissolves into the membrane. It should be noted that, at the pertinent tested concentration, there was no decrease in the optical density of the I1-treated cell suspensions, indicating that cell lysis did not occur. The same can be said of treatment with I2 and I3. Thus, we suggest that the collapse of $\Delta\Psi$ at the concentrations tested was caused by compound-mediated effects on the cell membrane rather than having occurred as a result of general cell lysis. Although I1, I2, and I3 all act on the membrane, only I1was disruptive to its structural integrity, causing leakage of large nucleotides, whereas I2 and I3 likely only cause small ions to be transported or released across its surface. Overall, molecules I1, I2, and I3 all decreased membrane potential, which in turn inhibited ATP production and depleted energy in the cell, leading to reduced viability.

Characterizing D1, D2, and D3, Potential Dissipaters of ΔpH

Similar to molecules I1–I3, we first assessed the effect of molecules D1, D2, and D3 on the reduction of INT (Figure 5A). All three molecules had adverse effects on cellular respiration, decreasing the production of formazan product, consistent with an action of dissipating PMF.

Additionally, D1, D2, and D3 also depleted cellular energy stores by causing a decrease in intracellular levels of ATP, however, to a lesser extent than I molecules. Because membrane potential, but not the pH gradient, is essential for the synthesis of ATP by the F1F0-ATPase (Kaim and Dimroth, 1998), it is not surprising that D1, D2, and D3 only decreased ATP levels by 37%, 16%, and 46%, respectively (Figure 5B). Finally, none of the dissipaters of ΔpH caused a significant leakage of cell constituents when tested at MIC values (Figure 5C), suggesting that they do not cause damage to the physical integrity of the membrane.

Characterizing I4, I5, I6, and I7: Other Molecules that Caused an Increase in $DiSC_3(5)$ Fluorescence

A number of molecules were uncovered in the HTS causing an increase in $DiSC_3(5)$ fluorescence but whose activity was not suppressed by an acidic external pH. We suspected that such molecules might inhibit cellular respiration, ultimately affecting membrane potential, or simply disrupt the membrane, allowing $DiSC_3(5)$ dye to be released.

Molecule I4 (Figure S4A) caused a dose-dependent increase in $DiSC_3(5)$ fluorescence (Figure S4B), but its activity was not

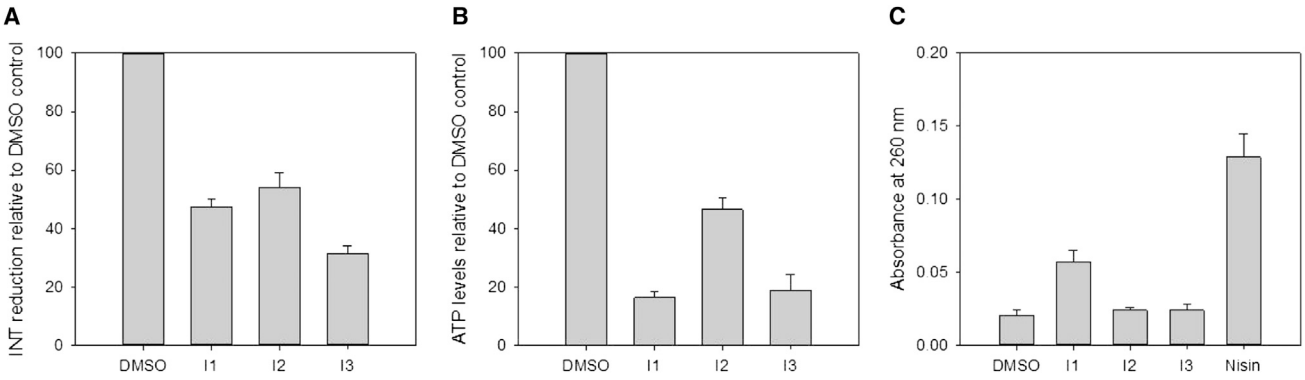

Figure 4. Effect of Potential Dissipaters of $\Delta\Psi$ at MIC Concentrations on Cellular Respiration, ATP Levels, and Membrane Integrity

(A) Effects of I1, I2, and I3 on the reduction of INT to its formazan product, which can be detected at an absorbance of 490 nm. Error bars represent the SEM of three replicates.

(B) Effects of compounds on intracellular ATP levels, measured by a luciferin-luciferase bioluminescence assay. Values are relative to DMSO control. Error bars represent the SEM of three replicates.

(C) Measure of leakage of cellular constituents at 260 nm with nisin as a positive control. Error bars represent the SEM of three replicates.

The MIC concentration of I1 is 8 μg/ml, I2 is 2 μg/ml, and I3 is 2 μg/ml.

potentiated upon a shift of the external pH to alkaline values. I4 did, however, suppress the activity of kanamycin against *S. aureus* by 8-fold (data not show), suggesting that I4 may inhibit cellular respiration. In fact, aminoglycoside bacterial uptake not only requires intact $\Delta\Psi$, but also electron flow through the membrane-associated respiratory chain (Taber et al., 1987). Expectedly, I4 led to decreased INT reduction as well as decreased intracellular ATP levels, as intact cellular respiration is required for both (Figures S4C and S4D). We also assessed its potential membrane-damaging properties by measuring for any loss of 260 nm absorbing material. I4 did not cause any significant release of cell constituents, suggesting it does not inhibit growth by permeabilizing the membrane of *S. aureus* (data not shown). Finally, cells treated with I4 had a significant reduction in their amount of staphyloxanthin pigment compared to untreated cells (Figure S4E). Staphyloxanthin synthesis has been shown to require intact cellular respiration (von Eiff et al., 2006). I4 may be driving *S. aureus* into fermentative growth, which would explain the decrease in ATP yield. Additionally, because pyruvate is shunted to support fermentation, less acetyl-CoA would enter the mevalonate pathway necessary for staphyloxanthin synthesis (Pelz et al., 2005). Interestingly, I4 synergized with I1–I3 and D1–D3 (Table S3), molecules that inhibit the generation of PMF, lending further support to the notion that I4 targets cellular respiration as a mechanism of action. In combination with these molecules, we would expect a respiration inhibitor to further deplete energy reserves leading to reduced viability.

Other active compounds, I5, I6, and I7 (Figure S5A) induced similar effects on *S. aureus*. All three caused significant increases in $DiSC_3$ fluorescence (Figure S5B). Unlike our specific dissipaters of $\Delta\Psi$, their antibacterial activities were not potentiated upon a pH shift to alkaline values, and they enhanced the activity of the kanamycin, instead of suppressing it. All three molecules did, however, cause a gross leakage of UV-absorbing material (Figure S5C), similar to nisin, suggesting that they may lead to structural disruption of the membrane. This permeabilization is likely the cause of the increase in $DiSC_3(5)$ dye, which is released in the medium and may also explain the observed enhanced activity of kanamycin, whose uptake would be accordingly facilitated. Interestingly, molecule I7 was structurally a bile salt, compounds known to disrupt cellular membranes (Ross et al., 2004). By disrupting membrane integrity, I5, I6, and I7 expectedly caused decreases in INT reduction and ATP levels (Table S4), as the respiratory chain and metabolic pathways within the cytoplasmic membrane would be destroyed. Further, the membrane damage caused by I5, I6, and I7 could be large enough to allow the leakage of large compounds, such as ATP. Finally, all three compounds were also synergistic with I1–I3 and D1–D3, the selective dissipaters of $\Delta\Psi$ and ΔpH, again likely due to their facilitated uptake into the cell and likely unrelated to an energetic mechanism.

Combinations of Molecules I1–I3 and D1–D3 Lead to Synergistic Interactions

Our overriding objective for the discovery of molecules that selectively dissipate $\Delta\Psi$ and ΔpH was their combination. We hypothesized that combining antibacterial compounds belonging to these two mechanistic classes would circumvent the compensatory responses in $\Delta\Psi$ and ΔpH that maintain PMF. Accordingly, we predicted synergistic, dose-sparing interactions from such combinations. We performed all possible combinations among molecules I1–I3 and molecules D1–D3 using antibacterial checkerboard methodology (White et al., 1996) against the highly problematic community-acquired methicillin-resistant strain of *S. aureus*, USA 300 (CA-MRSA USA300) (Figure 6). Here, we define synergy as having an FIC index of $\leq$ 0.5, additivity as 1–2, and antagonism as $\geq$2. In all cases, synergy was observed with FIC indices $\leq$0.5. The most potent synergies were observed for combinations of I2 with D2 and I3 with D3, each resulting in an FIC index of 0.25 (Figure 6). As controls, we also performed all combinations among the I molecules and on the other hand, among the D molecules; all combinations led to FIC indices ranging between 0.75–2 (data not shown), indicative of additive interactions.

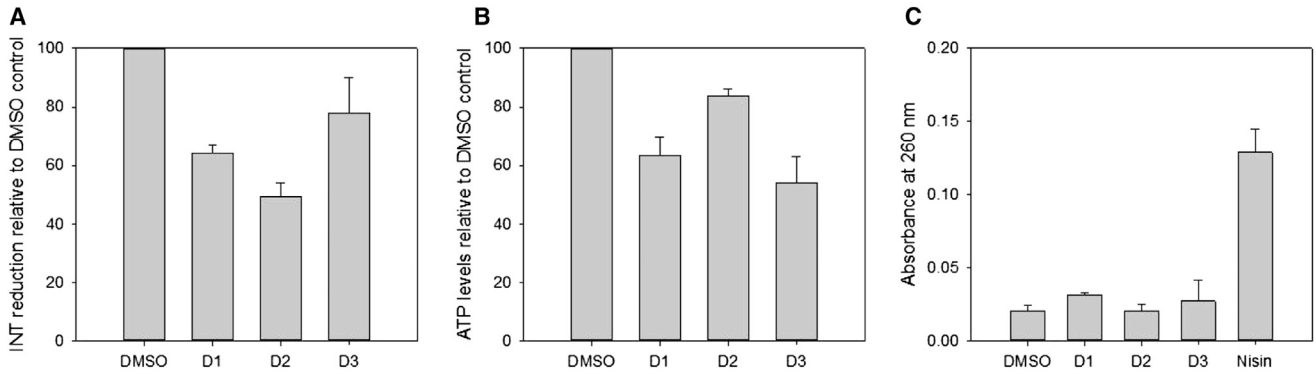

Figure 5. Effect of Potential Dissipaters of ΔpH at MIC Values on Cellular Respiration, ATP Levels, and Membrane Integrity

(A) Effects of D1, D2m and D3 on the reduction of INT to its formazan product, which can be detected at an absorbance of 490 nm. Error bars represent the SEM of three replicates.

(B) Effects of compounds on intracellular ATP levels, measured by a luciferin-luciferase bioluminescence assay. Values are relative to DMSO control. Error bars represent the SEM of three replicates.

(C) Measure of leakage of cellular constituents at 260 nm. Here, nisin is a positive control. Error bars represent the SEM of three replicates.

The MIC concentration of D1 is 32 μg/ml, D2 is 8 μg/ml, and D3 is 128 μg/ml.

Cytotoxicity Studies

The cytotoxic effects of compounds I1–I3 and D1–D3 against HeLa cells were evaluated by quantifying the release lactate dehydrogenase (LDH) upon cellular necrosis (Nachlas et al., 1960) (Figure 7A). In this assay, only two compounds, I1 and D1, significantly reduced cell viability by 41% and 47% at their antibacterial MIC values of 8 μg/ml and 32 μg/ml, respectively. At MIC concentrations, compounds I2 (MIC 2–4 μg/ml) and I3 (MIC 2–4 μg/ml) reduced cell viability by 9% and 6%, whereas D2 (MIC 8 μg/ml) and D3 (MIC 128 μg/ml) by 2% and 5%, respectively. Beyond the MIC values of the compounds, however, all but D3 showed significant cytotoxic effects on HeLa cells.

We next assessed whether toxicity at concentrations that lead to synergistic interactions could be minimized compared to toxicity of the compounds as antibacterial agents alone (Figure 7B). Overall, it was evident that the observed synergistic combinations would allow for reduced doses to be used, indeed minimizing cytotoxicity. We tested three of the nine combinations, I1 + D1, I2 + D2, and I3 + D3, at the concentration of each molecule that led to synergy for cytotoxicity effects (Figure 7B). Overall, toxicity of each compound could be reduced in combination, thus allowing for dose-sparing effects. For example, molecule I1 (that causes 41% toxicity alone) when combined with D1 (47% toxicity alone) at their effective synergistic concentrations led to 19% toxicity (Figure 7B). In combination, the activity of I1 is potentiated 4-fold by D1, reducing its cytotoxicity at that concentration to <25%, whereas D1 is potentiated 8-fold by I1, reducing its toxicity by over 20%. In other cases, such as with I2 and D2, displaying 9% and 2% cytotoxicity as single agents, respectively, resulted in very minimal cytotoxicity in combination (5%) (Figure 7B). Finally, as a single agent, I3 exhibited 10% toxicity at its MIC concentration and D3, 5% cytotoxicity. In combination, however, the total cytotoxicity at their effective synergistic concentrations was 7%, thus remaining almost negligible (Figure 7B). Overall, whereas all six compounds exhibited some moderate cytotoxicity, their combinations to achieve enhanced antibacterial efficacy allowed the ability to reduce cytotoxicity effects.

DISCUSSION

Bacteria establish and maintain an electrochemical gradient of protons across their cytoplasmic membrane, known as the PMF (Mitchell, 1966). This PMF is essential for a variety of critical bacterial processes, such as ATP synthesis, flagellar motility, and nutrient import. Collapse of the PMF inhibits these important functions and thus results in the loss of bacterial viability. A unique feature of the PMF is its composition of two components that continually work together to maintain homeostasis (Bakker and Mangerich, 1981). Dissipation of one component of the gradient is buffered by a counteracting increase in the other in order to maintain a constant value for the PMF. Nevertheless, most modern antibacterial discovery efforts purposely deprioritize molecules that disrupt membrane energetics. In the work reported here, we explore the potential of combining small molecules that perturb the $\Delta\Psi$ and ΔpH components of the PMF, with the underlying hypothesis that such agents should show advantageous synergy in combination.

Having established $DiSC_3(5)$ fluorescence as a robust assay to identify dissipaters of $\Delta\Psi$ and ΔpH, we screened a chemical library for small molecules modulators of $\Delta\Psi$ and ΔpH. Compounds specific to $\Delta\Psi$ and ΔpH were subsequently identified by their ability to suppress the activity of aminoglycosides or tetracyclines. Such molecules could also be modulated with changes in the external pH. This effort resulted in the identification of molecules I1, I2, and I3, which dissipate membrane potential, and D1, D2, and D3, which dissipate the pH gradient across the cell membrane of *S. aureus*. As expected, I1–I3 and D1–D3 all reduced the pool of intracellular ATP. We also uncovered a potential inhibitor of respiration, I4, as well as three membrane-damaging agents, I5, I6, and I7, which all led to increases in $DiSC_3(5)$ fluorescence.

Interestingly, Oyamada et al. (2006) have previously reported on molecule I1, discovered in an anucleate cell blue assay performed to identify type II topoisomerase inhibitors against *Escherichia coli*. In their in vitro follow-up, however, we note that I1 exhibited a very high IC_{50} toward purified gyrase and

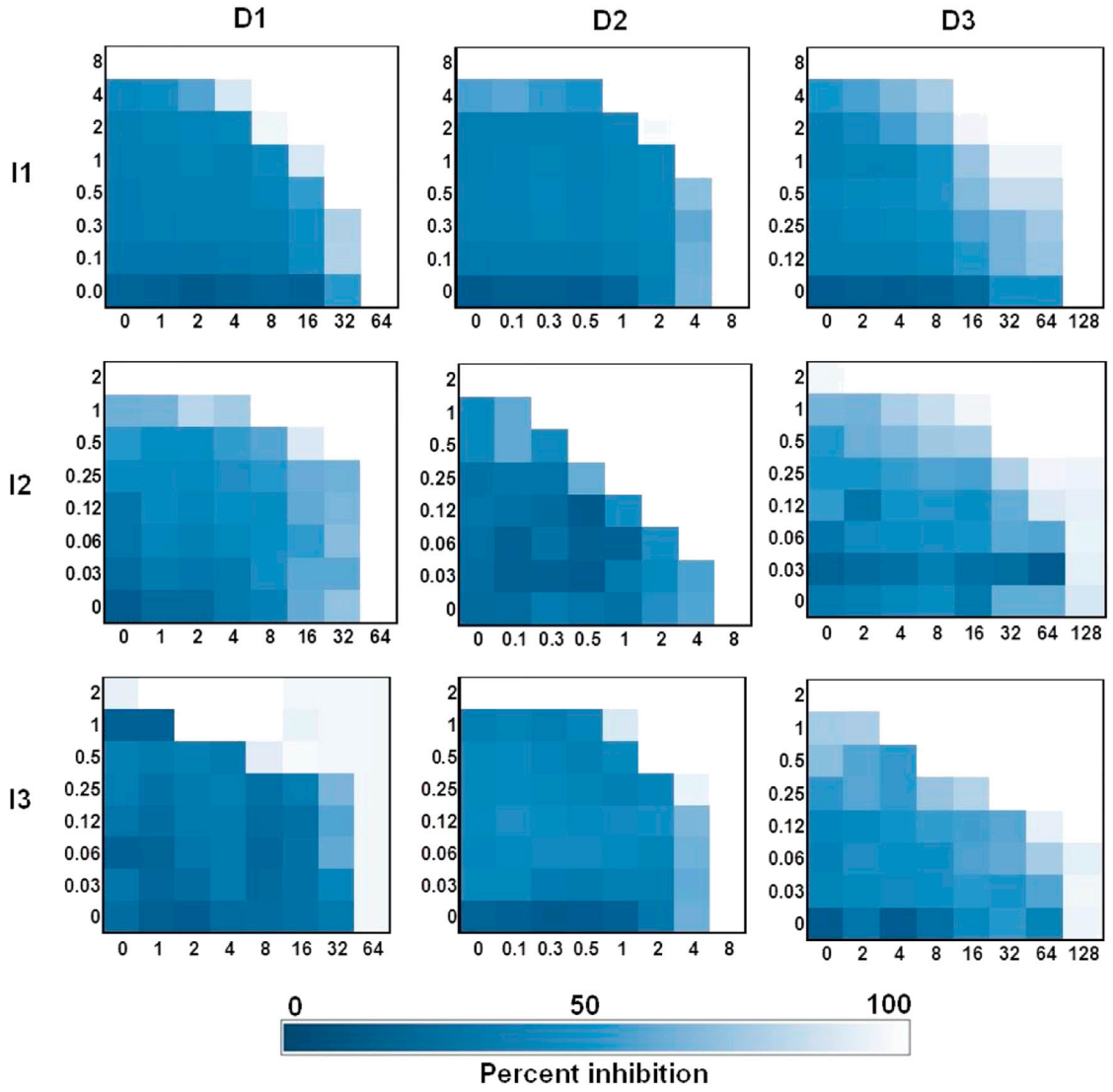

Figure 6. Combinations of Dissipaters of ΔΨ and ΔpH Exhibit Synergistic Interactions

Microdilution checkerboard analyses show all possible combined effects of molecules I1–I3 with molecules D1–D3 against CA-MRSA USA300 where the extent of inhibition is shown as a heat plot. In all cases, synergistic effects are evident and result in the following FIC indices: I1-D1 0.37, I1-D2 0.5, I1-D3 0.37, I2-D1 0.5, I2-D2 0.25, I2-D3 0.5, I3-D1 0.37, I3-D2 0.5, and I3-D3 0.25. FIC Index was calculated by the sum of the FIC of each compound, calculated as such; FIC = [X]/MIC_X, where [X] is the lowest inhibitory concentration of drug in the presence of the codrug.

topoisomerase IV, namely 50 μg/ml (171 μM) and >100 μg/ml (>342 μM), respectively. Further, molecule I3 is a natural product, known as agelasine found in marine sponges (*Agelas* sp.). Notably, no previous characterization of its antibacterial activity has been reported, but it has been characterized as a putative inhibitor of human Na/K-ATPase (Trachtenberg et al., 1981).

Importantly, in combination, synergistic interactions among our dissipaters of ΔΨ and dissipaters of ΔpH were observed and proved efficacious against MRSA. One advantage afforded by combination therapy over monotherapies is the ability to circumvent toxicity with dose-sparing concentrations of two-component therapy. Indeed, in the work presented here, cytotoxicity was significantly reduced through reductions in dose that were made possible by the synergies of I and D molecules when used in combination.

Although molecules that act on the membrane are often associated with toxicities, it is nevertheless clear that bacterial specificity is, in fact, attainable. The success stories of antibacterials such as daptomycin and telavancin, which depolarize the cytoplasmic membrane, reinforce the point that selective toxicity is achievable (Hurdle et al., 2011). In our case, molecules I1–I3 and D1–D3 displayed relatively low cytotoxicity at pertinent concentrations (i.e., those relating to antibacterial activity). Only I1 and D1 displayed high cytotoxicity against HeLa cells at very high concentrations, in many cases well above 32-fold their antibacterial inhibitory activity. Importantly, however, cytotoxicity was often negligible at MIC concentrations. In eukaryotic cells, the respiratory chain and resulting PMF is in the mitochondrial membrane instead of the cytoplasmic membrane. This distinct localization of the respiratory

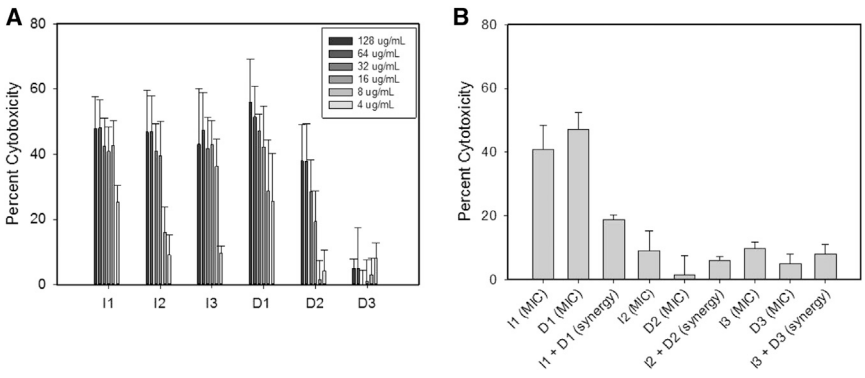

Figure 7. Cytotoxic Effects of Compounds I1, I2, and I3 as well as D1, D2, and D3 and Their Combinations on a HeLa Cell Line

(A) Cytotoxic effects of compounds I1–I3 and D1–D3 following exposure to different concentrations of compounds. Cell viability was assessed using LDH release method. All values are relative to the maximum LDH release control. Effect by the solvent DMSO was subtracted. Error bars represent the SEM of three replicates.

(B) Cytotoxic effects of individual compounds at MIC (antibacterial) concentrations and at concentrations that are effective (antibacterial) when used in the synergistic combinations indicated. Error bars represent the SEM of three replicates.

chain between eukaryotic and bacterial cells could partly explain the observed low toxicity (Wu et al., 2010). Nevertheless, their combinations allowed for dose-sparing effects and further lowered cytotoxicities.

A number of molecules impart bactericidal activity by collapsing the PMF, including a variety of antimicrobial peptides (Peters et al., 2010; Wilmes et al., 2011), which do so by forming pores and uncoupling agents that inhibit oxidative phosphorylation (Terada, 1990); fewer, however, selectively dissipate either component of the PMF (McAuliffe et al., 1998). Discriminating between decreases in the individual components of the PMF allows for a greater control of bacterial membrane energetics and gives an opportunity for collapsing the PMF via chemical combinations. In fact, targeting redundancy and homeostasis is a critical feature of combinatorial therapy and at the root of successful combination therapies (Cottarel and Wierzbowski, 2007; Fitzgerald et al., 2006).

We speculate that collapsing the PMF might be ideal as an antibacterial strategy against a variety of species. Compounds that collapse the PMF inhibit flagellar motility (Paul et al., 2008), preventing invasion (Nan et al., 2011) and swarming activities that eventually lead to biofilm formation (Ikonomidis et al., 2008). The PMF also plays a necessary role in protein excretion and the export of many toxic-secreted metabolites (Geller, 1991), which could be prevented by perturbing the PMF. Additionally, PMF-targeted molecules and their combinations could be expected to inhibit more efficiently dormant bacteria, a subpopulation of slow-growing or nongrowing microorganisms that play important roles in many persistent infections (Lewis, 2007). Dormant bacteria already have a reduced cellular metabolism, with a lowered but adequate proton motive force (Hurdle et al., 2011) and could thus be more susceptible to modulators of the PMF. Finally, many antibiotic efflux pumps are driven by the PMF (Paulsen et al., 1996), thus dissipaters of PMF could find utility as novel adjuvants to conventional antibiotics.

In the work reported here, we have presented a proof of concept for a rational and methodical strategy for the discovery of chemical combinations that block PMF in a synergistic manner. This method of achieving efficacy, although minimizing potential toxicities by targeting two interlinked components of a common pathway, provides a foundation for subsequent development of highly potent combinations and for the application to other compensatory pathways in the cell.

SIGNIFICANCE

Recently, we have seen a groundswell of concern over the lack of effective antibiotics to treat bacterial infection. The growing number of multidrug-resistant pathogens coupled with the retreat of the pharmaceutical sector from new antibiotic development has exacerbated this problem such that new, perhaps unconventional strategies are needed to meet these health challenges. Here, we report on an innovative approach to uncover synergistic combinations effective against resistant pathogens such as methicillin-resistant *Staphylococcus aureus*. Using a fluorescence-based high-throughput screen of *S. aureus*, we have identified selective dissipaters of either $\Delta\Psi$ or ΔpH, the components that make up the proton motive force (PMF). We reasoned that combinations of selective $\Delta\Psi$ and ΔpH perturbants would be uniquely synergistic because of a requirement in bacteria to maintain a constant PMF across the cytoplasmic membrane by balancing both components. We have identified three dissipaters of $\Delta\Psi$ and three dissipaters of ΔpH and provided evidence that strategically modulating $\Delta\Psi$ and ΔpH in concert via combinations leads to profound synergy with potent activity against MRSA. Additionally, we have shown that the synergy among these membrane-active compounds allows for considerable dose-sparing and as a result, lower toxicity. Indeed, modern antibacterial drug discovery has largely avoided membrane-active agents because of toxicity challenges. This work represents an alternative approach to tackle infectious pathogens and provides a methodical strategy to uncover synergistic antibacterial drug combinations.

EXPERIMENTAL PROCEDURES

Materials and Bacterial Strains

3,3′-Dipropylthiacarbocyanine iodide and all antibiotics used in the study were purchased from Sigma Aldrich. The strains used in the study are *S. aureus* (strain Newman strain) and CA-MRSA USA 300. Mueller Hinton Broth was used as the growth medium.

High-Throughput Screening for Molecules that Modulate PMF of *S. aureus*

Effects of compounds on the bioenergetics of the cytoplasmic membrane of *S. aureus* (strain Newman) were determined using the membrane potential-sensitive cyanine dye $DiSC_3(5)$ by a modification of the method of Epand

et al. (2010). Briefly, cultures of *S. aureus* were grown to exponential phase, washed three times, and resuspended in a buffer containing 10 mM potassium phosphate, 5 mM $MgSO_4$, and 250 mM sucrose (pH 7.0). After the final wash, pellets were resuspended in the same buffer to an optical density $(OD)_{600}$ of 0.085. The cells were loaded with 1 μM $DiSC_3(5)$ and allowed to stabilize before adding to assay plates containing compounds. Compounds were dispensed into 96-well assay plates (final concentration of 10 μM) using a Biomek FX liquid handler (Beckman Coulter). Cells were added using a μfill system (Biotek). Fluorescence was monitored at one time point using an EnVision plate reader (Perkin Elmer) at an excitation wavelength of 620 nm and an emission wavelength of 685 nm. The screen was completed in duplicate and each assay plate contained controls (16 wells total) including background DMSO controls, valinomycin, and nigericin controls. All raw data points were normalized to the mean of the middle two quartiles computed on an individual plate basis, to account for plate-to-plate variation, resulting in a ratio, where a high ratio indicates dissipation of $\Delta\Psi$ and a low ratio, dissipation of ΔpH. Positive and negative controls on each plate were used as checkpoints that the assay was running correctly. Hit compounds were selected based on an arbitrary cutoff of 1.4 for molecules that caused an increase in fluorescence and 0.25 for molecules that caused a decrease in fluorescence.

Counter Screen for Fluorescence Artifacts

Fluorescence artifacts were accounted for by measuring the fluorescence of the compounds that caused an increase in fluorescence on their own in assay buffer relative to DMSO controls. Conversely, compounds that caused a decrease in fluorescence were screened for their ability to quench the fluorescence of $DiSC_3(5)$ in assay buffer in the absence of cells.

Dose-Response Studies

Half-log serial dilutions of the hit compounds were prepared and aliquoted into assay plates. Fluorescence values were obtained in a similar manner as the screen. Curves were plotted on GraFit; any molecules with deviations from a clear dose-response relationship were eliminated.

MIC Determinations

Protocol for MIC determinations was based on Clinical and Laboratory Standards Institute (CLSI) guidelines. Plates were incubated at 37°C for 18 hr and optical density read at 600 nm. The MIC for the drug was the lowest concentration showing <10% growth.

INT Reduction Assay

S. aureus cells were grown from an overnight culture to exponential phase and washed and resuspended in 0.1 M potassium phosphate buffer (pH 7.5) to an optical density of 0.3 and kept on ice. In glass tubes, compound was added in buffer with 1 mM INT and 1 ml of cell in a total volume of 3 ml. Tubes were mixed vigorously and absorbance at 490 nm was read at 10 min intervals. Tubes were incubated at 30°C between reads.

ATP Levels

Protocol was adapted from Patton et al. (2006). ATP concentrations were determined using an ATP bioluminescent assay kit (Sigma) according to the manufacturer's instructions. Bioluminescence was measured using an EnVision plate reader (Perkin-Elmer).

Staphyloxanthin Levels

S. aureus cell culture at an OD 0.1 was treated with compound and grown at 37°C for 24 hr. Cells were centrifuged and pellets washed twice with PBS. Pigment was extracted in methanol, placing the samples in a 40°C water bath for 20 min. Samples were cooled and the absorbance of the extracted staphyloxanthin pigment was read at 450 nm and normalized to OD at 600 nm of the initial culture.

Checkerboard Analyses and FIC Index Determination

FICs were determined by setting up standard checkerboard broth microdilution assays using the conditions based on CLSI guidelines. Each drug was serially diluted at eight different concentrations to create an 8 × 8 matrix. At least three replicates were done for each combination and the means used for calculation. The FIC for each drug was calculated as the concentration of drug in the presence of codrug in a combination for a well showing <10% growth, divided by the MIC for that drug. The FIC index is the sum of the two FICs. Chemical-chemical interactions with an FIC index ≤ 0.5 were deemed synergistic.

Cytotoxicity Assays

Cytotoxicity experiments were performed using the CytoTox 96 nonradioactive cytotoxicity assay (Promega), which measures the release of lactate dehydrogenase (LDH) upon cellular necrosis. Briefly, HeLa cells were seeded at 10^4 cells per well of a 96-well plate in DMEM supplemented with 10% fetal calf serum and 1% Pen-Strep and incubated for 24–26 hr at 37°C/5% CO_2. Upon reaching 90%–95% confluence, cells were washed and stimulated with each compound in duplicate or triplicate at a concentration of 1 in 100 in complete DMEM. After 18 hr, LDH release was measured according to manufacturer's instructions. Each experiment was performed in triplicate, and all values are presented as relative to the maximum LDH release control, achieved by incubating unstimulated cells with 1× lysis buffer for 45 min prior to the measurement of LDH release.

SUPPLEMENTAL INFORMATION

Supplemental Information includes five figures and four tables and can be found with this article online at http://dx.doi.org/10.1016/j.chembiol.2013.07.006.

ACKNOWLEDGMENTS

This work was supported by grants from the Canadian Institutes of Health Research (MOP-81330 and Canada-UK Partnership on Antibiotic Resistance award 114045) and by a Canada Research Chair Award to E.D.B.

Received: June 7, 2013
Revised: July 11, 2013
Accepted: July 16, 2013
Published: August 22, 2013

REFERENCES

Altman, F.P. (1976). Tetrazolium salts and formazans. Prog. Histochem. Cytochem. *9*, 1–56.

Bakker, E.P., and Mangerich, W.E. (1981). Interconversion of components of the bacterial proton motive force by electrogenic potassium transport. J. Bacteriol. *147*, 820–826.

Balemans, W., Vranckx, L., Lounis, N., Pop, O., Guillemont, J., Vergauwen, K., Mol, S., Gilissen, R., Motte, M., Lançois, D., et al. (2012). Novel antibiotics targeting respiratory ATP synthesis in Gram-positive pathogenic bacteria. Antimicrob. Agents Chemother. *56*, 4131–4139.

Booth, I.R. (1985). Regulation of cytoplasmic pH in bacteria. Microbiol. Rev. *49*, 359–378.

Chopra, I. (2003). Antibiotic resistance in Staphylococcus aureus: concerns, causes and cures. Expert Rev. Anti Infect. Ther. *1*, 45–55.

Coates, A.R., and Hu, Y. (2008). Targeting non-multiplying organisms as a way to develop novel antimicrobials. Trends Pharmacol. Sci. *29*, 143–150.

Cottarel, G., and Wierzbowski, J. (2007). Combination drugs, an emerging option for antibacterial therapy. Trends Biotechnol. *25*, 547–555.

Epand, R.F., Pollard, J.E., Wright, J.O., Savage, P.B., and Epand, R.M. (2010). Depolarization, bacterial membrane composition, and the antimicrobial action of ceragenins. Antimicrob. Agents Chemother. *54*, 3708–3713.

Fitzgerald, J.B., Schoeberl, B., Nielsen, U.B., and Sorger, P.K. (2006). Systems biology and combination therapy in the quest for clinical efficacy. Nat. Chem. Biol. *2*, 458–466.

Garcerá, M.J., Elferink, M.G., Driessen, A.J., and Konings, W.N. (1993). In vitro pore-forming activity of the lantibiotic nisin. Role of protonmotive force and lipid composition. Eur. J. Biochem. *212*, 417–422.

Geller, B.L. (1991). Energy requirements for protein translocation across the Escherichia coli inner membrane. Mol. Microbiol. *5*, 2093–2098.

Gentry, D.R., Wilding, I., Johnson, J.M., Chen, D., Remlinger, K., Richards, C., Neill, S., Zalacain, M., Rittenhouse, S.F., and Gwynn, M.N. (2010). A rapid microtiter plate assay for measuring the effect of compounds on Staphylococcus aureus membrane potential. J. Microbiol. Methods *83*, 254–256.

Hawkey, P.M. (2008). Pre-clinical experience with daptomycin. J. Antimicrob. Chemother. *62*(*Suppl 3*), iii7–iii14.

Hu, Y., Shamaei-Tousi, A., Liu, Y., and Coates, A. (2010). A new approach for the discovery of antibiotics by targeting non-multiplying bacteria: a novel topical antibiotic for staphylococcal infections. PLoS ONE *5*, e11818.

Hurdle, J.G., O'Neill, A.J., Chopra, I., and Lee, R.E. (2011). Targeting bacterial membrane function: an underexploited mechanism for treating persistent infections. Nat. Rev. Microbiol. *9*, 62–75.

Ikonomidis, A., Tsakris, A., Kanellopoulou, M., Maniatis, A.N., and Pournaras, S. (2008). Effect of the proton motive force inhibitor carbonyl cyanide-m-chlorophenylhydrazone (CCCP) on Pseudomonas aeruginosa biofilm development. Lett. Appl. Microbiol. *47*, 298–302.

Kaim, G., and Dimroth, P. (1998). ATP synthesis by the F1Fo ATP synthase of Escherichia coli is obligatorily dependent on the electric potential. FEBS Lett. *434*, 57–60.

Keith, C.T., Borisy, A.A., and Stockwell, B.R. (2005). Multicomponent therapeutics for networked systems. Nat. Rev. Drug Discov. *4*, 71–78.

Lewis, K. (2007). Persister cells, dormancy and infectious disease. Nat. Rev. Microbiol. *5*, 48–56.

McAuliffe, O., Ryan, M.P., Ross, R.P., Hill, C., Breeuwer, P., and Abee, T. (1998). Lacticin 3147, a broad-spectrum bacteriocin which selectively dissipates the membrane potential. Appl. Environ. Microbiol. *64*, 439–445.

Mitchell, P. (1966). Chemiosmotic coupling in oxidative and photosynthetic phosphorylation. Biol. Rev. Camb. Philos. Soc. *41*, 445–502.

Nachlas, M.M., Margulies, S.I., Goldberg, J.D., and Seligman, A.M. (1960). The determination of lactic dehydrogenase with a tetrazolium salt. Anal. Biochem. *1*, 317–326.

Nan, B., Chen, J., Neu, J.C., Berry, R.M., Oster, G., and Zusman, D.R. (2011). Myxobacteria gliding motility requires cytoskeleton rotation powered by proton motive force. Proc. Natl. Acad. Sci. USA *108*, 2498–2503.

O'Neill, A.J., and Chopra, I. (2004). Preclinical evaluation of novel antibacterial agents by microbiological and molecular techniques. Expert Opin. Investig. Drugs *13*, 1045–1063.

Oyamada, Y., Ito, H., Fujimoto-Nakamura, M., Tanitame, A., Iwai, N., Nagai, K., Yamagishi, J., and Wachi, M. (2006). Anucleate cell blue assay: a useful tool for identifying novel type II topoisomerase inhibitors. Antimicrob. Agents Chemother. *50*, 348–350.

Patton, T.G., Yang, S.J., and Bayles, K.W. (2006). The role of proton motive force in expression of the Staphylococcus aureus Cid and lrg operons. Mol. Microbiol. *59*, 1395–1404.

Paul, K., Erhardt, M., Hirano, T., Blair, D.F., and Hughes, K.T. (2008). Energy source of flagellar type III secretion. Nature *451*, 489–492.

Paulsen, I.T., Brown, M.H., and Skurray, R.A. (1996). Proton-dependent multidrug efflux systems. Microbiol. Rev. *60*, 575–608.

Pelz, A., Wieland, K.P., Putzbach, K., Hentschel, P., Albert, K., and Götz, F. (2005). Structure and biosynthesis of staphyloxanthin from Staphylococcus aureus. J. Biol. Chem. *280*, 32493–32498.

Peters, B.M., Shirtliff, M.E., and Jabra-Rizk, M.A. (2010). Antimicrobial peptides: primeval molecules or future drugs? PLoS Pathog. *6*, e1001067.

Prakash Singh, M. (2006). Rapid test for distinguishing membrane-active antibacterial agents. J. Microbiol. Methods *67*, 125–130.

Ross, B.P., Braddy, A.C., McGeary, R.P., Blanchfield, J.T., Prokai, L., and Toth, I. (2004). Micellar aggregation and membrane partitioning of bile salts, fatty acids, sodium dodecyl sulfate, and sugar-conjugated fatty acids: correlation with hemolytic potency and implications for drug delivery. Mol. Pharm. *1*, 233–245.

Russell, J.B., and Houlihan, A.J. (2003). Ionophore resistance of ruminal bacteria and its potential impact on human health. FEMS Microbiol. Rev. *27*, 65–74.

Silver, L.L. (2011). Challenges of antibacterial discovery. Clin. Microbiol. Rev. *24*, 71–109.

Silverman, J.A., Perlmutter, N.G., and Shapiro, H.M. (2003). Correlation of daptomycin bactericidal activity and membrane depolarization in Staphylococcus aureus. Antimicrob. Agents Chemother. *47*, 2538–2544.

Taber, H.W., Mueller, J.P., Miller, P.F., and Arrow, A.S. (1987). Bacterial uptake of aminoglycoside antibiotics. Microbiol. Rev. *51*, 439–457.

Terada, H. (1990). Uncouplers of oxidative phosphorylation. Environ. Health Perspect. *87*, 213–218.

Trachtenberg, M.C., Packey, D.J., and Sweeney, T. (1981). In vivo functioning of the Na+, K+-activated ATPase. Curr. Top. Cell. Regul. *19*, 159–217.

Ultee, A., Kets, E.P., and Smid, E.J. (1999). Mechanisms of action of carvacrol on the food-borne pathogen Bacillus cereus. Appl. Environ. Microbiol. *65*, 4606–4610.

von Eiff, C., McNamara, P., Becker, K., Bates, D., Lei, X.H., Ziman, M., Bochner, B.R., Peters, G., and Proctor, R.A. (2006). Phenotype microarray profiling of Staphylococcus aureus menD and hemB mutants with the small-colony-variant phenotype. J. Bacteriol. *188*, 687–693.

White, R.L., Burgess, D.S., Manduru, M., and Bosso, J.A. (1996). Comparison of three different in vitro methods of detecting synergy: time-kill, checkerboard, and E test. Antimicrob. Agents Chemother. *40*, 1914–1918.

Wilmes, M., Cammue, B.P., Sahl, H.G., and Thevissen, K. (2011). Antibiotic activities of host defense peptides: more to it than lipid bilayer perturbation. Nat. Prod. Rep. *28*, 1350–1358.

Wu, M., Maier, E., Benz, R., and Hancock, R.E. (1999). Mechanism of interaction of different classes of cationic antimicrobial peptides with planar bilayers and with the cytoplasmic membrane of Escherichia coli. Biochemistry *38*, 7235–7242.

Wu, G., Wu, H., Fan, X., Zhao, R., Li, X., Wang, S., Ma, Y., Shen, Z., and Xi, T. (2010). Selective toxicity of antimicrobial peptide S-thanatin on bacteria. Peptides *31*, 1669–1673.

Yamaguchi, A., Ohmori, H., Kaneko-Ohdera, M., Nomura, T., and Sawai, T. (1991). Delta pH-dependent accumulation of tetracycline in Escherichia coli. Antimicrob. Agents Chemother. *35*, 53–56.

Zhanel, G.G., Calic, D., Schweizer, F., Zelenitsky, S., Adam, H., Lagacé-Wiens, P.R., Rubinstein, E., Gin, A.S., Hoban, D.J., and Karlowsky, J.A. (2010). New lipoglycopeptides: a comparative review of dalbavancin, oritavancin and telavancin. Drugs *70*, 859–886.

Zhang, J.H., Chung, T.D., and Oldenburg, K.R. (1999). A simple statistical parameter for use in evaluation and validation of high throughput screening assays. J. Biomol. Screen. *4*, 67–73.

